

Electronic supplementary information (ESI) for the manuscript:

Graphene oxide: an effective acid catalyst for the synthesis of polyoxymethylene dimethyl ethers from methanol and trioxymethylene

Ruiyi Wang,^{a,b} Zhiwei Wu,^a Zhangfeng Qin,^{*a} Chengmeng Chen,^c Huaqing Zhu,^a Jianbing Wu,^{a,b} Gang Chen,^b Weibin Fan^a and Jianguo Wang^{*a}

^a State Key Laboratory of Coal Conversion, Institute of Coal Chemistry, Chinese Academy of Sciences, P.O. Box 165, Taiyuan, Shanxi 030001, PR China. E-mail: qzhf@sxicc.ac.cn (Z. Qin); iccjgw@sxicc.ac.cn (J. Wang); Fax: +86-351-4041153; Tel: +86-351-4046092

^b University of Chinese Academy of Sciences, Beijing 100049, PR China

^c Key Laboratory of Carbon Materials, Institute of Coal Chemistry, Chinese Academy of Sciences, Taiyuan, Shanxi 030001, PR China

1. More Experimental Details:

1.1. Catalyst preparation

Materials used: Graphite powder (Aladdin); H₂SO₄ (Xilong Chem. Co., Ltd, China); KMnO₄ (Kermel Chem. Reagent CO., Ltd, China); NaNO₃ (Kermel Chem. Reagent Co., Ltd, China); H₂O₂ (30%, Dong Fang Chem. Co., Ltd, China); carbon nanotube and active carbon (Nanjing XFNANO Materials Tech. Co., Ltd, China); 1,4-dihydroxybenzene, 1,4-benzoquinone, 1,4-dicarboxybenzene, o-hydroxybenzoic acid, phenylsulfonic acid and sulfosalicylic acid (Aladdin); tetramethoxysilane, ethanol and NaBH₄ (Sinopharm Chemical Reagent Co., Ltd).

Graphene oxide (GO): GO was prepared by a modified Hummers' method,¹ followed by exfoliation in aqueous solution under sonicating for 2 h. Briefly, graphite powder (10 g) and sodium nitrate (5 g) were mixed with sulfuric acid (230 mL, 98 wt.%) in an ice bath under agitation. Potassium permanganate (30 g) was then added slowly and the mixture was kept at 35 ± 2 °C for 30 min. After that, deionized water (460 mL) was gradually added, with violent effervescence. The water bath was then heated to 98 °C and maintained at this temperature for 40 min. The resultant bright-yellow suspension was diluted and further treated with H₂O₂ solution (30 mL, 30%). The suspension was centrifuged and carefully washed to clean out the residual salts, and then dewatered by vacuum drying at 50 °C to obtain the GO powder. Finally, the GO catalyst was obtained by exfoliation of the GO powder in aqueous solution by sonicating for 2 h and then dried in vacuum at 60 °C. The yield of GO (Y_{GO}) on the basis of carbon content prepared in this way is about 70%, as calculated by $Y_{GO} = (m_{GO} \times c_C / m_{\text{graphite}}) \times 100\%$, where m_{graphite} and m_{GO} are the masses of graphite used and GO obtained, respectively, and c_C is the mass composition of carbon element in GO (47.98%).

GO-COOH, GO preserved with -COOH groups: GO-COOH was obtained by selectively poisoning the hydroxyl groups through silylation with tetramethoxysilane.² Briefly, GO (0.5 g) was dispersed in toluene (20 mL), followed by dropwise addition of tetramethoxysilane (50 μ L); the mixture was stirred at 35 °C for 12 h. After that, the resulting materials was washed with ethanol to remove the unreacted silylation agents and then subjected to filtration and drying in vacuum at 60 °C.

GO-OH, GO preserved with -OH groups: GO-OH was obtained through reduction with NaBH₄, in which the carbonyl and carboxyl groups on GO surface were selectively removed.³ Briefly, GO (0.5 g) were added to a suspension of NaBH₄ (15 mmol) in THF (100 mL) at room temperature; the mixture was then stirred vigorously until the evolution of gas ceased.

After that, the mixture was stirred for another 2 h in argon atmosphere and then the excess solvent and other impurities were removed through washing with hot ethanol for three cycles. The GO-OH product was finally isolated from the mixture by filtration and dried in vacuum at 60 °C.

Sulfonated active carbon and carbon nanotubes (S-AC and S-CNTs): S-AC and S-CNTs were obtained by treating AC and CNTs in the concentrated sulphuric acid, respectively. Briefly, AC or CNTs (0.5 g) was heated in H₂SO₄ (30 mL, 98 wt%) at 150 °C for 6 h. The suspension was centrifuged and the solid product was then washed with distilled water and finally dried at 60 °C to get the sulfonated S-AC or S-CNTs.

GO-HT, desulfurated GO: To get GO-HT, GO (1.0 g) was heated in deionized water (50 mL) at 150 °C for 12 h; the suspension was centrifuged and the solid product was washed with distilled water and finally dried at 100 °C.

1.2. Catalyst characterization

The powder X-ray diffraction (XRD) patterns of catalyst samples were collected on a Rigaku MiniFlex II desktop X-ray diffractometer with CuK α radiation source. The measurements were made in the 2θ range from 5° to 80° with a scanning rate of 4 ° min⁻¹.

The scanning electron microscopy (SEM) images to characterize the surface morphologies of the catalyst samples were acquired on a field emission scanning electron microscope (FESEM, JSM 7001-F, JEOL, Japan), with energy dispersive X-ray spectroscopy (EDX, QX200).

The X-ray photoelectron spectroscopy (XPS) spectra were taken on a Thermo ESCALAB 250 instrument, with an Al K α monochromator X-rays source ($h\nu = 1486.6$ eV);

approximate 150 mg of the powder sample was compressed into a wafer for the measurements.

The Fourier transform infrared (FT-IR) spectra were measured on a Bruker Tensor 27 FT-IR spectrometer. The catalyst sample was first pressed into a pellet with KBr and the IR spectra were then recorded at room temperature in the range of 400–4000 cm^{-1} with a resolution of 4 cm^{-1} .

The atomic force microscope characterization (AFM) was conducted for GO sheets on a scanning probe microscope (Tip mode, frequency of 0.803 Hz, Veeco NanoScope IIIa Multimode, DI, USA); the sample was precisely prepared by depositing the hydrosol of GO on freshly cleaved mica surface.

Raman spectra were recorded on a Renishaw inVia Raman spectrometer; a 514.5 nm Ar-ion laser was employed as the exciting source.

The contents of elements (C, H, O, N, S) in the catalyst samples were determined by the elemental microanalysis (EA, vario MICRO cube, Elemental).

1.3. Catalytic tests

The synthesis of PODE_n was carried out in a stainless steel autoclave of 100 mL lined with teflon. Typically, 3.2 g methanol (MeOH), 4.5 g trioxymethylene (TOM) and 0.385 g GO were loaded into the autoclave; the reaction mixture was heated to 120 °C and kept at 120 °C for 10 h under vigorous stirring.

The products after reaction, including DMM, PODE_n , MF, and FA, and unreacted reactants, were measured with decane as an internal standard by two gas chromatographs: one is Shimadzu GC-2014C equipped with a FID detector and DB-1 capillary column for

determining PODE_n, DMM, TOM, MeOH, etc.; the other one is Shimadzu GC-14B equipped with a TCD detector and Porapak T packed column for MeOH, FA, MF, DMM, water, etc. In any case, the mass balance accounts for 95–105%.

The conversions of DMM (x_{MeOH}) and TOM (x_{TOM}) are determined by

$$x_{\text{MeOH}} = (n_{\text{MeOH,feed}} - n_{\text{MeOH,product}}) / n_{\text{MeOH,feed}} \times 100\%,$$

$$x_{\text{TOM}} = (n_{\text{TOM,feed}} - n_{\text{TOM,product}} - n_{\text{FA,product}}/3) / n_{\text{TOM,feed}} \times 100\%,$$

and the mass selectivity to each product is determined by

$$s_i = m_{i,\text{product}} / \sum m_i \times 100\%.$$

For an example, the mass selectivity to PODE₂₋₈ is

$$s_{\text{PODE}_{2-8}} = m_{\text{PODE}_{2-8}} / \sum m_i \times 100\%,$$

where m_i is the mass of species i ($m_{\text{PODE}_{2-8}}$, the mass of PODE₂₋₈) in the products and $\sum m_i$ is the mass of all the liquid products collected after the reaction test.

2. More Results of Catalyst Characterization and Reaction Tests:

2.1. More results for the characterization of GO

The SEM image of GO and AFM image of individual GO sheets are shown in Fig. S1 and Fig. S2, respectively, which indicate that the as-prepared GO is in flimsy sheets with a thickness of 1.42 nm. According to the elemental analysis (Table S1), the mass fractions of C, O, S, H and N elements in GO are 47.98%, 47.52%, 2.36%, 2.02%, and 0.12%, respectively; the heteroatoms, especially O, S and H, constitute the various acid groups.

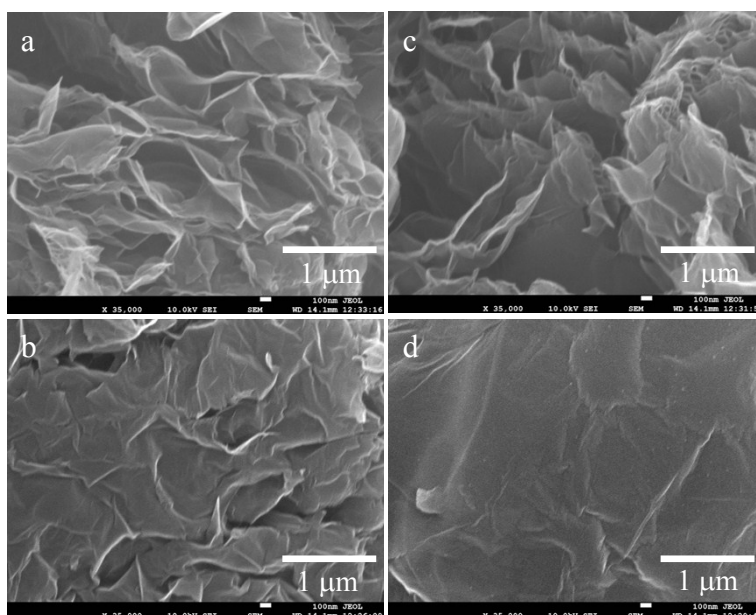


Fig. S1 SEM images of (a) GO, (b) GO-COOH, (c) GO-OH, and (d) GO-HT.

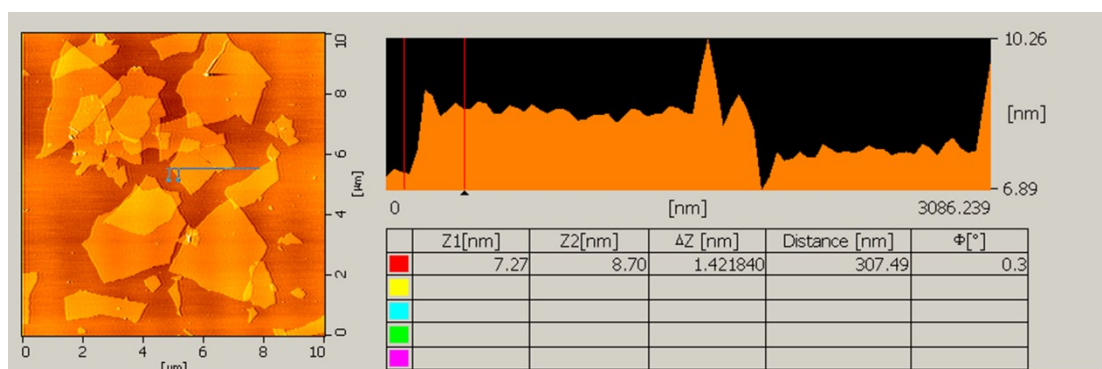


Fig. S2 AFM image of individual GO sheets, showing a thickness of 1.42 nm.

Table S1 Contents of various elements in mass percentage of GO and those preserved with certain groups

Catalyst	C	O	S	H	N	Si
GO	47.98	47.52	2.36	2.02	0.12	--
GO-OH	47.53	47.63	2.01	2.67	0.16	--
GO-COOH	33.19	35.24	1.99	2.39	0.15	27.04
GO-HT	54.25	42.34	0.36	2.88	0.17	--

As displayed in Fig. S3, the XRD pattern of graphite shows a very intensive peak at 26.69° , whereas GO displays an intense peak at 12.22° which is typical for C (001), suggesting that the interlayer space is expanded from 0.338 nm of graphite to 0.704 nm of GO, because of the insertion of various oxygen-containing functional groups.

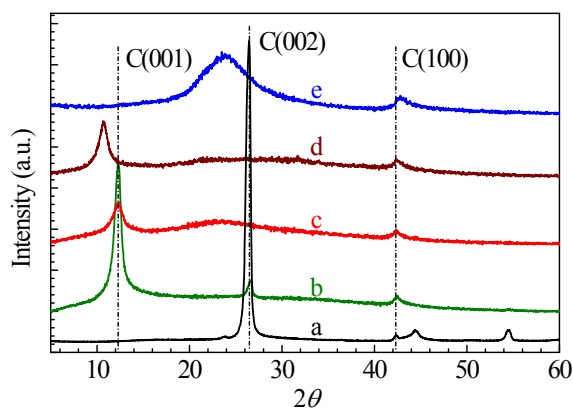


Fig. S3 XRD patterns of (a) Graphite, (b) GO, (c) GO-COOH, (d) GO-OH, and (e) GO-HT.

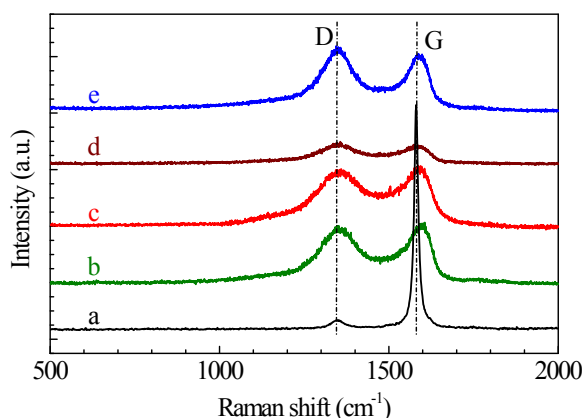


Fig. S4 Raman spectra of (a) graphite, (b) GO, (c) GO-COOH, (d) GO-OH, and (e) GO-HT.

Raman spectroscopy was also used to figure out the structural variations during the chemical processing of graphene oxide from graphite. As displayed in Fig. S4, the graphite shows a single G peak at 1582 cm^{-1} corresponding to the first order scattering of the E_{2g} mode, whereas broad D and G bands are both observed for GO, indicating that abundant hydroxyl and epoxide groups are attached on the carbon basal plane.⁴

2.2. Effect of reaction temperature, reaction time and catalyst amount on PODE_n synthesis

First, the effect of operation conditions on the reactant conversion and product selectivity in the synthesis of PODE_n from MeOH and TOM over GO are considered, as given in Table S2. With the increase of reaction time from 0.5 to 10 h at 120 °C, the conversion of TOM and the mass selectivity to PODE₂₋₈ climb from 40.2% to 92.8% and 0 to 30.9%, respectively, and then level off with further extension of the reaction time.

With the elevation of reaction temperature from 75 to 150 °C (with a reaction time of 10 h), the conversion of TOM is increased monotonously from 53.9% to 96.1%. However, a maximum mass selectivity of 30.9 % to PODE₂₋₈ is attained at 120 °C. At a lower temperature, e.g. 75 °C, the product is dominated by DMM with a selectivity of 92.6% and PODE_n ($n > 2$) is not detected, whereas at a higher temperature, e.g. 150 °C, the mass selectivity to PODE₂₋₈ is decreased to 17.3%. The synthesis of PODE_n involves a series of reactions such as TOM dissociation to FA, condensation of FA with MeOH to DMM, PODE_n chain propagation, Tishchenko reaction of FA to MF and so on. Current results then imply that a temperature below 120 °C is probably insufficient for the TOM dissociation and PODE_n chain propagation, whereas a temperature above 120 °C may promote the PODE_n dissociation and other side reactions.

Meanwhile, the amount of GO catalyst also has an influence on the PODE_n synthesis. When the amount of GO used in the PODE_n synthesis is 1 wt.%, DMM appears as the major product. The conversion of TOM and the mass selectivity to PODE₂₋₈ increases with the amount of catalyst and level off when the catalyst amount used reaches 5 wt.%.

Table S2 Effect of the reaction temperature, reaction time and catalyst amount used on the reactant conversion and product selectivity for the synthesis of PODE_n from MeOH and TOM over GO ^a

Temperature (°C)	Time (h)	GO amount (wt.%)	Conversion (%)		Mass selectivity (%)			
			MeOH	TOM	DMM	PODE ₂₋₈	MF	FA
120	0.5	5.0	48.4	40.2	94.3	0.0	0.0	5.7
120	1	5.0	58.2	64.6	57.7	9.9	31.0	1.4
120	6	5.0	59.7	70.4	22.7	10.3	13.3	53.7
120	8	5.0	69.1	80.9	26.1	14.5	9.7	46.7
120	10	5.0	90.3	92.8	21.1	30.9	0.2	47.8
120	15	5.0	90.8	89.9	22.0	29.3	2.9	45.8
75	10	5.0	42.4	53.9	92.6	0.0	0.0	7.4
100	10	5.0	82.7	75.8	69.7	4.1	14.3	11.9
120	10	5.0	90.3	92.8	21.1	30.9	0.2	47.8
150	10	5.0	91.9	96.1	59.9	17.3	12.7	10.1
120	10	1.0	74.9	68.8	86.2	5.3	5.2	3.3
120	10	2.0	87.9	85.0	59.5	3.6	25.7	11.1
120	10	3.0	90.1	86.8	53.8	10.4	11.3	24.4
120	10	5.0	90.3	92.8	21.1	30.9	0.2	47.8
120	10	10.0	91.4	94.2	24.4	30.3	0.2	45.0

^a The feed MeOH/TOM molar ratio is 2. The mass selectivity to a given product is defined as its weight divided by the weight of all products.

All these suggest that a temperature of 120 °C, a reaction time of 10 h and a GO catalyst amount of 5 wt.% are probably the optimal reaction conditions for the synthesis of PODE_n from MeOH and TOM with a MeOH/TOM molar ratio of 2; under such conditions, the

conversion of TOM and the mass selectivity to PODE₂₋₈ reach 92.8% and 30.9%, respectively. Interestingly, a high selectivity to PODE₂₋₈ is generally accompanied with a relatively high selectivity to FA, which may prove that the dissociation of trioxymethylene is a crucial step in the process of PODE_n synthesis, in accord with the results of Wu, Li, and coworkers.^{5,6}

2.3. Characterization of GO catalysts selectively preserved with certain groups

The SEM images of GO derivatives, viz., GO-OH, GO-COOH and GO-HT, are also displayed in Fig. S1. Obviously, GO derivatives exhibit a similar morphology as GO; they all take a plicated layer structure. These suggest that the macroscopic structure and morphology of GO are not changed after the modification; the difference between GO and its derivatives in the catalytic performance should be mainly ascribed to the alteration of functional groups in GO upon various treatments.

The alteration of functional groups in GO upon various treatments also has a reflection on the XRD patterns of GO derivatives, as illustrated in Figure S3. GO displays an intense diffraction peak at 12.56° which is typical for C (001), suggesting an interlayer space of 0.704 nm because of the insertion of various oxygen-containing functional groups. The diffraction peak position of GO-COOH is basically unchanged. However, GO-OH shows an interlayer space of 0.823 nm (10.75°), according with the results reported by Shin and coworkers.³ When GO is hydrothermally treated, this diffraction peak has disappeared in the XRD pattern of GO-HT, whereas a broad peak at 23.78° emerges, implying that most of the functional groups, especially the -SO₃H groups, are removed after the treatment under hydrothermal conditions.⁷

Raman spectroscopy is also performed to figure out the structural variation of GO upon

various treatments, such as the reduction with NaBH_4 , silylation with tetramethoxysilane and hydrothermal treatment of GO, as displayed in Fig. S4. For GO, the D band at 1353 cm^{-1} corresponds to the vibrations of carbon atoms at defect sites and the G band at 1596 cm^{-1} refers to the vibrations of carbon atoms in the ideal graphitic lattice. Red shifts are observed for GO-OH, GO-COOH and GO-HT, which are consistent with the elimination of partial oxygen-containing groups ($-\text{OH}$, $-\text{COOH}$ and $-\text{SO}_3\text{H}$) upon corresponding treatments.⁸ Moreover, after the subsequent hydrothermal treatment of GO, the I_D/I_G value for GO-HT is increased from 0.94 to 1.12, indicating the presence of abundant structural defects.

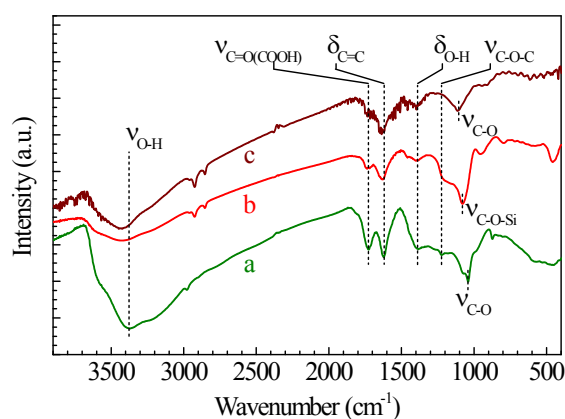


Fig. S5 FT-IR spectra of GO with selectively preserved groups: (a) GO; (b) GO-COOH; and (c) GO-OH.

Fourier transform infrared (FT-IR) spectroscopy is very effective to differentiate the carboxyl and hydroxyl groups in GO and its derivatives. As illustrated in Fig. S5, the FT-IR spectrum of GO shows a wide hydroxyl stretching vibration in carboxyl, phenol, and/or intercalated H_2O ($\nu_{\text{O-H}}$) at 3400 cm^{-1} as well as C=O stretching vibration in carbonyl and carboxyl groups ($\nu_{\text{C=O}}$) at 1720 cm^{-1} . The adsorption peak at 1626 cm^{-1} is assigned to the skeletal vibrations of un-oxidized aromatic graphitic domains ($\delta_{\text{C=C}}$), whereas the peaks at 1388 , 1218 , and 1043 cm^{-1} are attributed to the carboxyl C=O deformation vibrations ($\delta_{\text{O-H}}$), epoxy and/or ether type C-O-C ($\nu_{\text{C-O-C}}$), and alkoxy C-O stretching vibrations ($\nu_{\text{C-O}}$),

respectively.¹ In comparison with GO, a new peak at 1079 cm⁻¹ assigned to C–O–Si stretching appears in the FT-IR spectrum of GO-COOH,² whereas the peak at 1388 cm⁻¹ for the carboxyl C=O deformation vibrations ($\delta_{\text{O-H}}$) has disappeared and the peak intensity at 3400 cm⁻¹ for $\nu_{\text{O-H}}$ is also largely reduced. It suggests that the –OH groups on the GO surface are successfully poisoned by silylating with tetramethoxysilane, whereas the carboxyl groups are still retained ($\nu_{\text{C=O}}$ at 1722 cm⁻¹) on GO-COOH.⁹ On the other hand, for GO-OH, the disappearance of the peak at 1722 cm⁻¹ for C=O confirms that the –COOH group has been selectively removed by NaBH₄, leaving the hydroxyl groups remained on GO-OH surface.

The changes in the sulfonic groups and the carboxyl and hydroxyl groups of GO derivatives (GO-COOH, GO-OH and GO-HT) in comparison with that of GO are also evidenced by the X-ray photoelectron spectroscopy (XPS), as displayed Fig. S6.

There are no peaks observed for S and N elements in the survey XPS spectra (Fig. S6(I)), due to the relatively low content of S and N on the surface of GO and its derivatives determined by elemental analysis (Table S1). In the high-resolution N 1s XPS spectra (Fig. S6(II)), the peak for nitrogen at 399.6 eV is very weak, consistent with its very low content. The peaks for sulfur are clearly observed around 167 eV in the high-resolution S 2p XPS spectra of GO, GO-COOH and GO-OH (Fig. S6(III)), close to that of –SO₃H in Amberlyst-15;¹⁰ however, such a peak for sulfur has disappeared in GO-HT, proving that the sulfonic groups in GO can be successfully removed by the hydrothermal treatment. Meanwhile, the signal for Si element is only observed in the XPS spectrum of GO-COOH obtained by the silylation of GO with tetramethoxysilane (Fig. S6(I)).

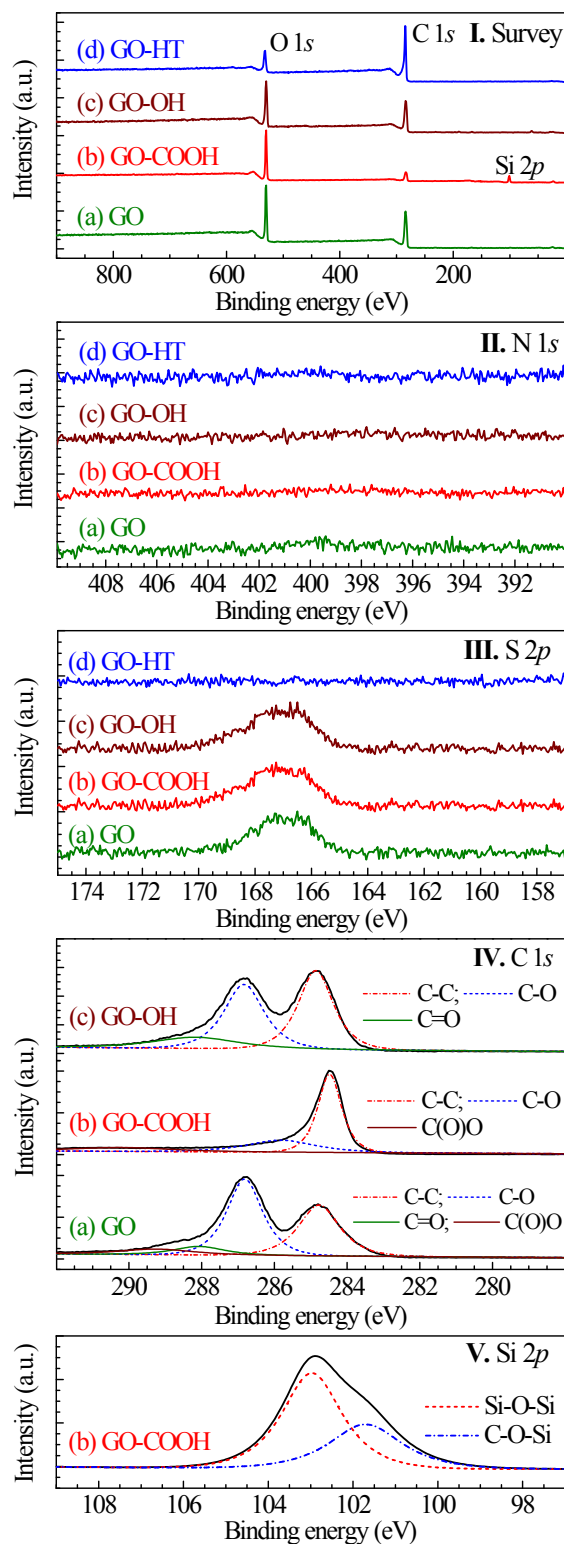


Fig. S6 (I) Survey XPS spectra; (II) N 1s XPS spectra; (III) S 2p XPS spectra; (IV) C 1s XPS spectra; and (V) Si 2p XPS spectra. For samples: (a) GO; (b) GO-COOH; (c) GO-OH; and (d) GO-HT.

A high resolution of C 1s XPS spectra further reveal the variance of the carboxyl and hydroxyl groups of GO-COOH and GO-OH in comparison with that of GO (Fig. S6(IV)). The C 1s spectrum for GO can be fitted into four peaks at 285, 287, 288 and 290 eV, which are corresponding to C–C species, C–O group, C=O group, and O=C–O group, respectively.^{2,11}

For GO-COOH, the peak intensity for C–OH species is greatly reduced due to the silylation of GO with tetramethoxysilane, whereas the signal for COOH is retained and a peak at 101.6 eV in the Si 2p spectra for C–O–Si was detected (Fig. S6(V)), consistent with its high content of silicon element (Table S1). For GO-OH, on the other hand, the disappearance of O=C–O group signal at 290 eV indicates that the –COOH group is successfully removed by the reduction with NaBH₄, consistent with the FT-IR results.

The dissolubility and stability of GO and its derivatives in the reaction system were also examined. GO and its derivatives were first dispersed in MeOH and ultrasonicated for 30 min; the suspension mixture then stood quietly for 1.0 h and their pictures were taken, as displayed in Fig. S7. GO is still uniformly dispersed in MeOH after standing for 1.0 h; however, GO-OH, GO-COOH and GO-HT may precipitate easily.

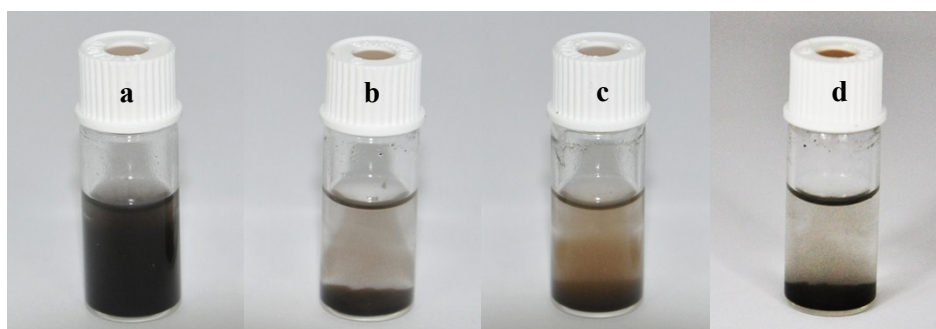


Fig. S7 Picture of (a) GO, (b) GO-COOH, (c) GO-OH and (d) GO-HT dispersed in MeOH after ultrasound for 30 min and then settled statically for 1.0 h

Such a phenomenon indicates that the oxygen-containing functionalities on the surface of GO may not only act as the active sites in the PODE_n synthesis but also serve as surfactants to stabilize the GO suspension, which increases the contacting probability between GO and reactants and enhance the reaction activity. However, as illustrated latter, GO as a heterogeneous catalyst is easily separated from the suspension mixture by filtration after the reaction and used for the next run without any further treatment.

2.4. Effects of various solvents and raw reactants on the synthesis of PODE_n

The effects of various solvents and raw reactants on the synthesis of PODE_n were also considered, as shown in Table S3. When MeOH and TOM are used as the raw materials to synthesize PODE_n (Entry 1), water is produced as a by-product, which may promote the hydrolysis of PODE_n and is then prejudicial to the formation of long chain PODE_n . As anticipated, water as an additional solvent exhibits a negative effect on production of PODE_{2-8} (Entry 2).

On the other hand, when toluene as an inert solvent is used, the reactant conversion is hardly influenced, whereas the selectivity to PODE_{2-8} is moderately enhanced (Entry 3). Toluene as a solvent is effective to extract ether products, which may prevent them from further hydrolysis and then shift the reaction to long chain PODE_n . In fact, when DMM and TOM were used as the raw materials to synthesis PODE_n (Entry 4), the mass selectivity to long chain PODE_n products is largely enhanced, as this reaction does not produce water; the mass selectivity PODE_{2-8} reaches 85.9% and even certain longer chain products is also detected. These may suggest that DMM and TOM are more suitable as the raw materials to get high quality PODE_n .⁵

Table S3 Effect of the solvent and raw reactant on the PODE_n synthesis catalyzed by GO ^a

Entry	Solvent	Conversion (%)			Mass selectivity (%)					
		MeOH	DMM	TOM	DMM	PODE ₂₋₈	PODE _{>8}	MeOH	MF	FA
1	none	90.3	non ^b	92.8	21.1	30.9	0.0	inappl. ^c	0.2	47.8
2	water	91.5	non ^b	92.4	39.2	4.6	0.0	inappl. ^c	4.6	51.6
3	toluene	81.9	non ^b	91.6	38.5	38.0	0.0	inappl. ^c	2.6	20.9
4	none	non ^b	84.9	94.6	inappl. ^c	85.9	0.7	1.3	0.0	12.1
5	none	2.0	non ^b	non ^b	0	0	0	inappl. ^c	100	0
6	none	non ^b	non ^b	55.6	0	0	0	0	3.0	97.0

^a The reactions were carried out at 120 °C for 10 h, with a catalyst amount of 5 wt.% and initial MeOH/TOM or DMM/TOM molar ratio of 2; the amount of solvent when used is 50 wt.% on the basis of the mass of all reactants. The mass selectivity to a given product is defined as its weight divided by the weight of all products.

^b “non” means that the corresponding substance is not a reactant added in the initial reaction mixture and then its conversion cannot be determined for such a reaction test.

^c “inappl.” means that the corresponding substance appears also as a reactant in the initial reaction mixture and the selectivity to it is then inapplicable to such a reaction test.

Meanwhile, when MeOH is taken as the sole reactant, GO is rather catalytically inactive and only 2% of it is converted to MF (Entry 5, Table S3). On the other hand, when TOM is used as the sole reactant, its conversion and the selectivity to FA reach 55.6% and 97.0%, respectively, whereas the mass selectivity to MF is only 3% (Entry 6). These further prove that GO as a catalyst is very effective for the dissociation of TOM to FA and further chain propagation with DMM and MeOH to form PODE₂₋₈, whereas it is less active for the methanol oxidation and Tishchenko reaction to form the side products such as MF.

2.5. Catalytic stability and reusability of GO in PODE_n synthesis

To test the catalytic stability and reusability of GO in PODE_n synthesis, GO was separated from the mixture after reaction by filtration and used for the next run without any further treatment. As illustrated in Fig. S8, GO as the catalyst is deactivated slightly after being reused for five cycles; the conversion of TOM is decreased from 92.8% to 85.2%, whilst the mass selectivity to PODE_{2-8} is also decreased from 30.9% to 16.3%. Such impairment should be attributed to the slow elimination of functional groups under the harsh hydrothermal reaction conditions.^{12,13} Liao and coworkers also reported that GO could be reduced to single-layer graphene in water at 95 °C.¹⁴ Fortunately, the oxygen-containing functionalities served as the active sites can be easily refurbished with concentrated sulphuric acid. As also displayed in Fig. S8, when the deactivated GO is treated in the concentrated sulphuric acid at 80 °C for 4 h, the conversion of TOM and the mass selectivity to PODE_{2-8} are reclaimed to 89.5% and 30.6%, respectively.

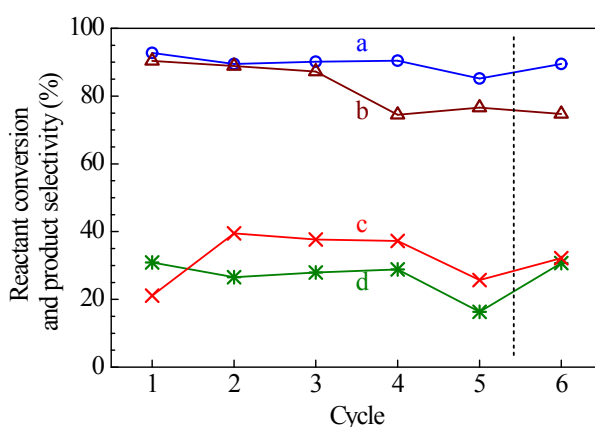


Fig. S8 Reusability of GO as a catalyst in the synthesis of PODE_n from MeOH and TOM: (a) TOM conversion; (b) MeOH conversion; (c) selectivity to DMM; (d) selectivity to PODE_{2-8} . The reactions were carried out at 120 °C for 10 h, with a catalyst amount of 5 wt.% and initial MeOH/TOM molar ratio of 2. After each test, the catalyst is re-used in next run upon a simple centrifugation separation. For the 6th cycle, the GO catalyst was subject to an activation process through a treatment in the concentrated sulphuric acid at 80 °C for 4 h.

2.6. Comparison of GO with other catalysts preciously reported in PODE_n synthesis

The catalytic performance of GO used in this work are also compared with that of some other typical heterogeneous catalysts previously reported in PODE_n synthesis, when MeOH and TOM or DMM and TOM are used as the raw materials, as given in Table S4.

Table S4 Comparison between GO used in this work and some other typical heterogeneous catalysts preciously reported in PODE_n synthesis

Entry	Catalyst	Reactants	Temperature (°C)	Time (h)	x_{TOM} (%)	$s_{\text{PODE}_{2-8}}$ (%)	Reference
1	GO	MeOH, TOM	120	10	92.8	30.9	this work
2	SO ₄ ²⁻ /Fe ₂ O ₃ -SiO ₂	MeOH, TOM	130	2	81.9	34.4	6
3	PVP-stabilized heteropolyacids	MeOH, TOM	140	4	95.7	52.5	15
4	HMCM-22 zeolite	MeOH, TOM	120	10	39.8	65.1	16
5	GO	DMM, TOM	120	10	94.6	85.9	this work
6	[PY-BS][HSO ₄ ⁻] ion liquid	DMM, TOM	150	10	90.4	92.3	17
7	HZSM-5 zeolite	DMM, TOM	120	0.75	85.3	88.5	5
8	CT175 cation resins	DMM, TOM	90	0.5	89.0	95.7	18

As there are many factors that affect the catalytic activity and product selectivity, it is very difficult to give a quantitative comparison in their activity without a kinetic analysis under the same reaction conditions. However, the data in Table S4 do illustrate that GO used in this work exhibits relatively high conversion of raw materials and high selectivity to PODE₂₋₈ at relatively low reaction temperature. GO prepared by the modified Hummers' method as a catalyst performs excellently in the synthesis of PODE_n from MeOH and TOM; with a catalyst amount of 5 wt.% and initial MeOH/TOM molar ratio of 2, the conversion of

TOM and selectivity to PODE₂₋₈ reach 92.8% and 30.9%, respectively, after reaction at 120 °C for 10 h. Such results suggest that GO can be a potential catalyst for the synthesis of PODE_n, which are also meaningful for the extension of GO application in other catalytic synthesis processes.

Notes and references

- 1 C. Chen, Q. Zhang, M. Yang, C. Huang, Y. Yang and M. Wang, *Carbon*, 2012, **50**, 3572–3584.
- 2 H. Yao, L. Jin, H. Sue, Y. Sumi and R. Nishimura, *J. Mater. Chem. A*, 2013, **1**, 10783–10789.
- 3 H. Shin, K. Kim, A. Benayad, S. Yoon, H. Park, I. Jung, M. Jin, H. Jeong, J. Kim, J. Choi and Y. Lee, *Adv. Function. Mater.*, 2009, **19**, 1987–1992.
- 4 E. Lam, J. H. Chong, E. Majid, Y. Liu, S. Hrapovic, A. Leung and J. Luong, *Carbon*, 2012, **50**, 1033–1043.
- 5 J. Wu, H. Zhu, Z. Wu, Z. Qin, L. Yan, B. Du, W. Fan and J. Wang, *Green Chem.*, 2015, **17**, 2353–2357.
- 6 H. Li, H. Song, L. Chen and C. Xia, *Appl. Catal. B*, 2015, **165**, 466–476.
- 7 S. Pei and H. Cheng, *Carbon*, 2012, **50**, 3210–3228.

- 8 Y. Zhou, Q. Bao, L. A. Tang, Y. Zhong and K. Loh, *Chem. Mater.*, 2009, **21**, 2950–2956.
- 9 M. Ju, I. Jeon, K. Lim, J. Kim, H. Choi, I. Choi, Y. Eom, Y. Kwon, J. Ko, J. Lee, J. Baek and H. Kim, *Energy Environ. Sci.*, 2014, **7**, 1044–1052.
- 10 F. Liu, J. Sun, L. Zhu, X. Meng, C. Qi and F. Xiao, *J. Mater. Chem.*, 2012, **22**, 5495–5502.
- 11 X. Fan, W. Peng, Y. Li, X. Li, S. Wang, G. Zhang and F. Zhang, *Adv. Mater.*, 2008, **20**, 4490–4493.
- 12 H. Wang, Q. Kong, Y. Wang, T. Deng, C. Chen, X. Hou and Y. Zhu, *ChemCatChem*, 2014, **6**, 728–732.
- 13 S. Zhu, C. Chen, Y. Xue, J. Wu, J. Wang and W. Fan, *ChemCatChem*, 2014, **6**, 3080–3083.
- 14 K. Liao, A. Mittal, S. Bose, C. Leighton, K. Mkhoyan and C. Macosko, *ACS nano*, 2011, **5**, 1253–1258.
- 15 X. Fang, J. Chen, L. Ye, H. Lin and Y. Yuan, *Sci. China Chem.*, 2015, 1–8.
- 16 J. Cao, H. Zhu, H. Wang, L. Huang, Z. Qin, W. Fang and J. Wang, *J. Fuel Chem. Techno.*, 2014, **42**, 986–993.

- 17 Q. Wu, M. Wang, Y. Hao, H. Li, Y. Zhao and Q. Jiao, *Ind. Eng. Chem. Res.*, 2014, **53**, 16254–16260.
- 18 L. Wang, W. Wu, T. Chen, Q. Chen and M. He, *Chem. Eng. Commun.*, 2013, **201**, 709–717.